A meshfree approach for the Timoshenko beam

Felipe P. dos Santos[1], Enzo Marino[2], Lapo Gori[1]

[1]*Dept. of Structural Engineering, Federal University of Minas Gerais*
Avenida Antonio Carlos, 6627, 31270-901, Belo Horizonte/MG, Brazil
felipe-pereira@ufmg.br, lapo@dees.ufmg.br
[2]*Dept. of Civil and Environmental Engineering, University of Florence*
Via di Santa Marta, 3 - 50139 Firenze, Italy
enzo.marino@unifi.it

Abstract. Besides the finite element method, there are a number of numerical methods for the analysis of shear deformable beams available in the literature, developed to improve the convergence properties and the shear-locking behaviour exhibited by the finite element method. This paper investigates the application of a meshfree method of the family of Smoothed Point Interpolation Methods (S-PIM) to the analysis of the Timoshenko beam. Numerical simulations are also presented, in order to illustrate preliminary results in terms of convergence properties obtained with a peculiar type of shape function, among the ones of the S-PIM approach.

Keywords: Smoothed point interpolation methods (S-PIMs), Edge-based, Timoshenko beam

1 Introduction

In various engineering fields there are many applications using meshfree methods, among which the family of smoothing point interpolation methods (S-PIMs) are relatively recent. The S-PIMs encompasses the node-based smoothed point interpolation method (NS-PIM) proposed by Liu et al. [1], the cell-based smoothed point interpolation method (CS-PIM) that first appeared in Zhang and Liu [2] and the edge-based smoothed point interpolation method (ES-PIM) proposed in the work of Liu and Zhang [3]. A rich discussion concerning to the mentioned S-PIMs can be found in Liu and Zhang [4]. In general, the applications of meshfree methods including S-PIMs are addressed for two and three dimensional problems, however applications for one dimensional problems are also available in the literature, e.g., Liu [5], Hale [6], Du et al. [7] and He et al. [8].

In this paper the ES-PIM will be investigated on the analysis of the Timoshenko beam. An error comparison of ES-PIM with the linear FEM is also presented. The ES-PIM simulations were performed using the open-source software INSANE [1].

2 Timoshenko beam

The Timoshenko beam model adopted in this paper is based on the following assumptions: no elongation along the beam axis, no torsion around the beam axis and plane bending, with the bending plane aligned with a principal axis of the cross section. Furthermore, the strains are assumed to be small, and the beam is assumed to be initially straight. With these assumptions, the kinematics of the model (Fig. 1a) is characterised by the deflection v of the beam axis and by the rotation θ of the cross-sections, resulting in the following strain measures:

$$\gamma_{xy} := \frac{\partial v}{\partial x} - \theta, \quad \omega := \frac{\partial \theta}{\partial x}, \tag{1}$$

---

[1]INSANE stands for *INteractive Structural ANalysis Environment System*. For more information the reader may refer to: `http://www.insane.dees.ufmg.br`.

(a) Timoshenko beam section   (b) Edge-based smoothing domains (2D case)
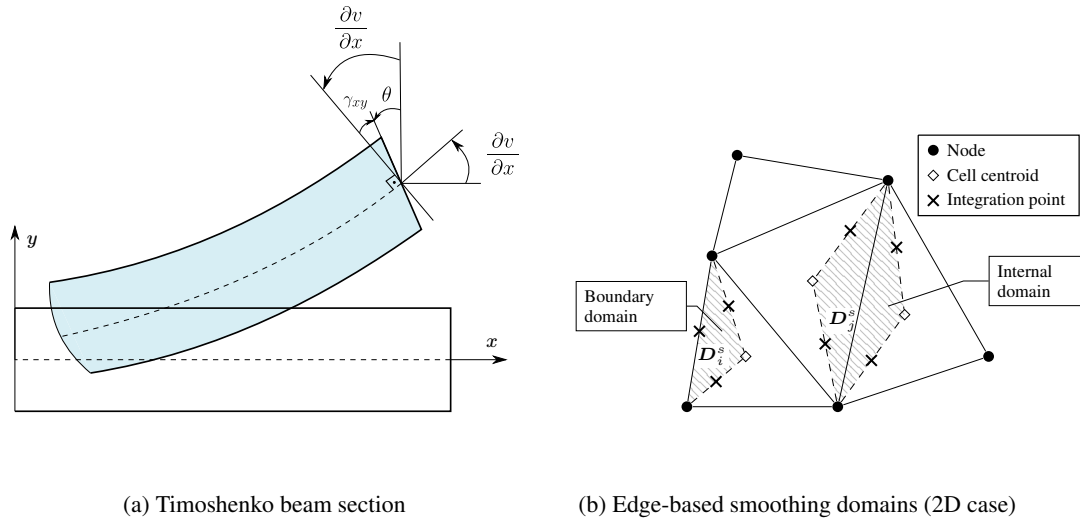
Figure 1

where ω is the curvature and γ_{xy} is the shear strain.

The model is governed by the following differential equations, that constitute the strong form of the Timoshenko beam:

$$\frac{\partial}{\partial x}\left(EI\frac{\partial\theta}{\partial x}\right) + k_s GA\left(\frac{\partial v}{\partial x} - \theta\right) = 0 \quad \text{and} \quad \frac{\partial}{\partial x}\left[GA_s\left(\frac{\partial v}{\partial x} - \theta\right)\right] = -q_y(x), \tag{2}$$

where E is the Young modulus, G the shear modulus, A the cross sectional area, I the second inertia moment of area, k_s the shear correction factor, $q_y(x)$ the load acting along the beam.

3 Edge based smoothed point interpolation method (ES-PIM)

The ES-PIM was originally proposed by Liu and Zhang [3] for 2D applications. Their method is based on point interpolation shape functions and on a tesselation of the domain into smoothing domains, constructed over the edges of triangular background cells (Fig. 1b). Such smoothing domains are used to transform the gradients of the field variables into boundary integrals using the Green theorem (see Liu [9] for further details). In the present one dimensional application each smoothing domain $\boldsymbol{D}_n^s$ is constructed over the edges illustrated in Fig. 2, and the integration points used to perform the boundary integration over each domain coincide with the nodes. It is worth noticing that the proposed approach is a sort of degeneration of the 2D approach proposed by Liu and Zhang [3]. As discussed in section 3.1, the gradients of the field variables are assumed to be constant within each smoothing domain. For a point of interest $\boldsymbol{x}$ the field variables are approximated as follows:

$$v(\boldsymbol{x}) = \sum_{i=1}^{sd} \phi_i^v(\boldsymbol{x})v_i, \quad \theta(\boldsymbol{x}) = \sum_{i=1}^{sd} \phi_i^\theta(\boldsymbol{x})\theta_i, \tag{3}$$

where sd is the number of support nodes selected in a local support domain, ϕ_i^v and ϕ_i^θ are the shape functions created for a support node i for the displacements and rotations, respectively, and v_i and θ_i are the nodal values of $v(\boldsymbol{x})$ and $\theta(\boldsymbol{x})$ at $\boldsymbol{x} = \boldsymbol{x}_i$.

In the present paper, the shape function ϕ_i are generated with three different strategies: the Point Interpolation Method (PIM), the Radial Point Interpolation Method (RPIM), and the Radial Point Interpolation Method with polynomial reproduction (RPIMp); details on these strategies can be found in Liu [9].

In order to evaluate the support nodes used to construct the shape functions at each integration point, two different approaches are proposed in this paper. With the so-called L2-scheme, the support domain at each integration point is constituted by the two nodes of the edge where the point belongs to (Fig. 3a). The L32-scheme considers,
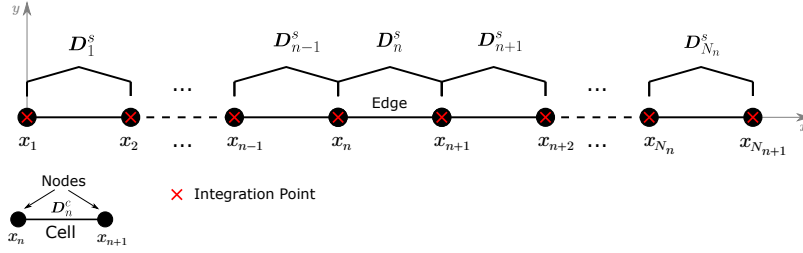
Figure 2. Edge-based smoothing domain (1D case)

(a) L2-scheme for support nodes selection for an interior point of interest. Interior or boundary cell

(b) L32-scheme for support nodes selection for an interior point of interest
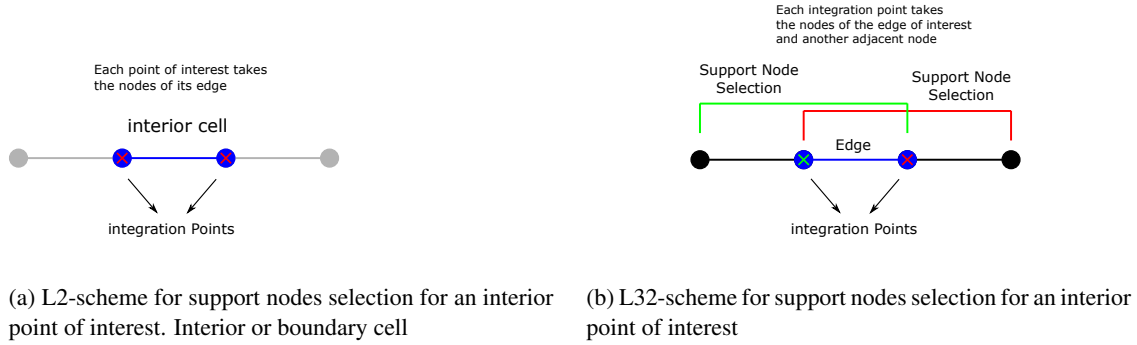
Figure 3

for each integration point, the two nodes of the edge where the point belongs to, and an additional node from the neighbour edge (Fig. 3b). For integration points on the boundary of the model, the L32-scheme degenerate to the L2-scheme. It is noted that these schemes are analogous to the T-schemes proposed by Liu [9] for 2D applications.

3.1 Weakened-weak form

As pointed out in the previous section, S-PIM methods are based on a smoothing technique for the gradients of the field variables, that results in the so-called weakened-weak form Liu [10], i.e., a weak form with a reduced order of continuity of its functions. From eq. (2) one can derive the following weak form through a weighted residual method:

$$\int_0^L \delta\omega EI\omega dx + \int_0^L \delta\gamma_{xy}GA_s\gamma_{xy}dx = \int_0^L \delta v q_y(x)dx + [\delta v GA_s(\gamma_{xy})]|_0^L + [\delta\theta EI(\omega)]|_0^L, \tag{4}$$

where $\delta\theta$ and δv are the rotation and displacement test functions respectively, $A_s = k_s A$ and the following quantities were defined:

$$\delta\gamma_{xy} := \frac{\partial\delta v}{\partial x} - \delta\theta, \quad \delta\omega := \frac{\partial\delta\theta}{\partial x}. \tag{5}$$

The S-PIMs are characterised by a smoothing operation on the derivatives over the smoothing domains. Inspired by the proposal presented in Liu and Zhang [3] and Liu [5] adapted for an one dimensional approach, the weakened-weak form of eq. (4) will be achieved. First of all, only its left hand side will be considered, then, the smoothing operation takes place and the Green's divergence theorem is applied converting all the domain integrals of the gradients where the field variables appeared into boundary integrals. Hence, this one dimensional case assumes the form (Liu [5]):

$$\widetilde{\frac{\partial v}{\partial x}} = \frac{1}{l_i}\int_{\Gamma_i} v(x)\,n(x)dx, \quad \widetilde{\frac{\partial\theta}{\partial x}} = \frac{1}{l_i}\int_{\Gamma_i} \theta(x)\,n(x)dx, \tag{6}$$

where ℓ_i is the length of the ith smoothing domain, $n(x)$ the normal outward unit vector, Γ_i the boundary of the smoothing domain $\boldsymbol{D}_i^s$. The above procedure will be applied in the quantities defined in eq. (1) and eq. (5), in order to do that, the mentioned quantities are replaced by their smoothed versions based on eq. (6) as follows:

$$\widetilde{\delta\omega} = \frac{1}{l_i^s} \int_{\Gamma_i^s} \delta\theta\, n(x)dx, \quad \widetilde{\omega} = \frac{1}{l_i^s} \int_{\Gamma_i^s} \theta\, n(x)dx, \tag{7}$$

$$\widetilde{\delta\gamma_{xy}} = \frac{1}{l_i^s} \int_{\Gamma_i^s} \delta v\, n(x)dx - \delta\tilde{\theta}, \quad \widetilde{\gamma_{xy}} = \frac{1}{l_i^s} \int_{\Gamma_i^s} v\, n(x)dx - \tilde{\theta}, \tag{8}$$

Aiming at the simplest approach, $\delta\tilde{\theta}$ and $\tilde{\theta}$ will be defined as the central values of the functions $\delta\theta$ and θ, assumed to be constant, in the smoothing domain where for the edge-based approach is the midpoint of the edge:

$$\delta\tilde{\theta} \approx \delta\theta_{\text{mid}}, \quad \tilde{\theta} \approx \theta_{\text{mid}}. \tag{9}$$

Introducing the shape functions in eq. (7) and eq. (8) and replacing the derivatives of the shape functions with their smoothed versions, the following smoothed strain measures are obtained:

$$\widetilde{\omega}(x_k) = \sum_{i=1}^{sd} \widetilde{\phi}_{i,x}^\theta \theta_i, \qquad \widetilde{\gamma}(x_k) = \sum_{i=1}^{sd} \left(\widetilde{\phi}_{i,x}^v v_i - \phi_i^\theta \theta_i \right), \tag{10}$$

where x_k is the central point of the smoothing domain and the smoothed shape functions are expressed as:

$$\widetilde{\phi}_{i,x}^\theta(x_k) = \frac{1}{l_i^s} \int_{\Gamma_i^s} \phi_i^\theta\, n(x)dx, \quad \widetilde{\phi}_{i,x}^v(x_k) = \frac{1}{l_i^s} \int_{\Gamma_i^s} \phi_i^v\, n(x)dx. \tag{11}$$

Writing the smoothed strain measures in matrix form it results in:

$$\{\widetilde{\varepsilon}(x_k)\} = \begin{bmatrix} \widetilde{\omega}(x_k) \\ \widetilde{\gamma}(x_k) \end{bmatrix} = \sum_{i=1}^{sd} \begin{bmatrix} 0 & \widetilde{\phi}_{i,x}^\theta \\ \widetilde{\phi}_{i,x}^v & -\phi_i^\theta \end{bmatrix} \begin{bmatrix} v_i \\ \theta_i \end{bmatrix} = [\boldsymbol{B}_i(x_k)][\boldsymbol{u}_p], \tag{12}$$

where $\boldsymbol{u}_p$ is the vector of unknowns and the matrix $\boldsymbol{B}_i$ is defined as:

$$[\boldsymbol{B}_i(x_k)] := \begin{bmatrix} 0 & \widetilde{\phi}_{i,x}^\theta \\ \widetilde{\phi}_{i,x}^v & -\phi_i^\theta \end{bmatrix}. \tag{13}$$

It is important to highlight that the components of $\boldsymbol{B}_i$ matrix are constants in the smoothing domain. At this point, the matrix version of the left hand side of eq. (4) can be expressed as:

$$\int_D \delta\varepsilon(x) \underbrace{\begin{bmatrix} EI & 0 \\ 0 & GA_s \end{bmatrix}}_{[\boldsymbol{E}]} \varepsilon(x)dx \rightarrow \sum_{k=1}^{N_s} l_k \delta\widetilde{\varepsilon}(x_k)[\boldsymbol{E}]\widetilde{\varepsilon}(x_k), \tag{14}$$

where l_k is the length of the kth smoothing domain, N_s is the number of smoothing domains in the discretisation and $[\boldsymbol{E}]$ is the constitutive matrix. Therefore the problem equation assumes the form:

$$\sum_{k=1}^{N_s} \sum_{i=1}^{sd} l_k \begin{pmatrix} \delta v_i & \delta \theta_i \end{pmatrix} [\boldsymbol{B}_i^T][\boldsymbol{E}][\boldsymbol{B}_i] \begin{pmatrix} v_i \\ \theta_i \end{pmatrix}. \tag{15}$$

The stiffness matrix of the kth smoothing domain is expressed as follows[2]:

$$\boldsymbol{K}_k = \sum_{i=1}^{sd} l_k [\boldsymbol{B}_i^T][\boldsymbol{E}][\boldsymbol{B}_i]. \tag{16}$$

3.2 Numerical simulations

In this section, the numerical simulations of a cantilever Timoshenko beam (Fig. 4) performed with the proposed ES-PIM strategy are illustrated. The results are presented in terms of displacement and rotation along the beam axis, and are compared with the exact solution and with the linear FEM (Fig. 5 and Fig. 6). The results are also presented in terms of an error norm.
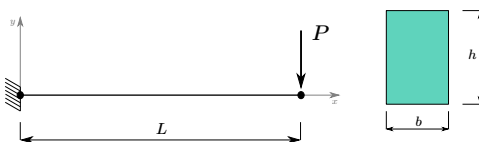
Figure 4. Cantilever beam with a point load at its tip

The parameters adopted for the numerical simulations are: Young's modulus $E = 2 \times 10^{11}$ N/m^2, Poisson's ratio $\nu = 0.3$, rectangular cross section with dimensions $b = 0.2$ m and $h = 0.3$ m, beam length $L = 10$ m, form factor $k = 5/6$ and $P = 10000$ N.

The meshfree shape functions were constructed with the PIM, RPIM and RPIMp methods; the RPIM and RPIMp methods are based on an exponential radial function Liu [9] with a shape parameter equal to 1, and the polynomial reproduction in the RPIMp shape functions was obtained with two polynomial terms. The FEM was simulated using one integration point to avoid the shear locking problem. The error was estimated with the following expression:

$$e = \left[\frac{\displaystyle\sum_{i=1}^{N_n}(v_i^{ref} - v_i^{num})^2 + \sum_{i=1}^{N_n}(\theta_i^{ref} - \theta_i^{num})^2}{\displaystyle\sum_{i=1}^{N_n}(v_i^{ref})^2 + \sum_{i=1}^{N_n}(\theta_i^{ref})^2} \right]^{\frac{1}{2}}, \tag{17}$$

where $\boldsymbol{v}_i^{ref}$ and $\boldsymbol{\theta}_i^{ref}$ are the reference solution for the displacements and rotations at node i, respectively, $\boldsymbol{v}_i^{num}$ and $\boldsymbol{\theta}_i^{num}$ gather the numerical solution for the displacement and rotation at node i, respectively, and N_n is the total number of the field nodes used in the problem domain.

The results obtained in terms of displacement and rotation along the beam axis are illustrated in Fig. 5, for a mesh with 5 equally spaced nodes, and in Fig. 6, for a mesh with 11 equally spaced nodes. The numerical

---

[2]The right hand side of eq. (4) is treated in a standard process.

(a) Displacements. Mesh with 5 Nodes

(b) Rotations. Mesh with 5 Nodes

Figure 5

(a) Displacements. Mesh with 11 Nodes

(b) Rotations. Mesh with 11 Nodes
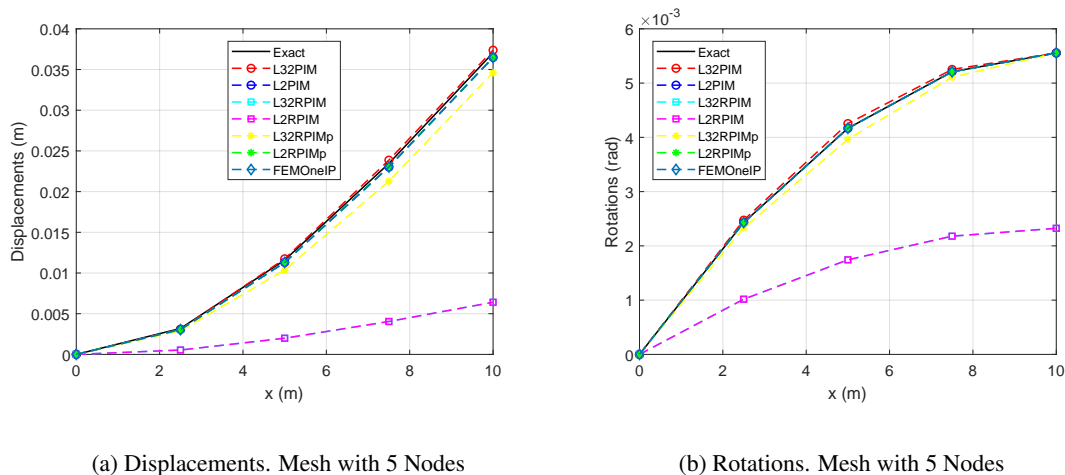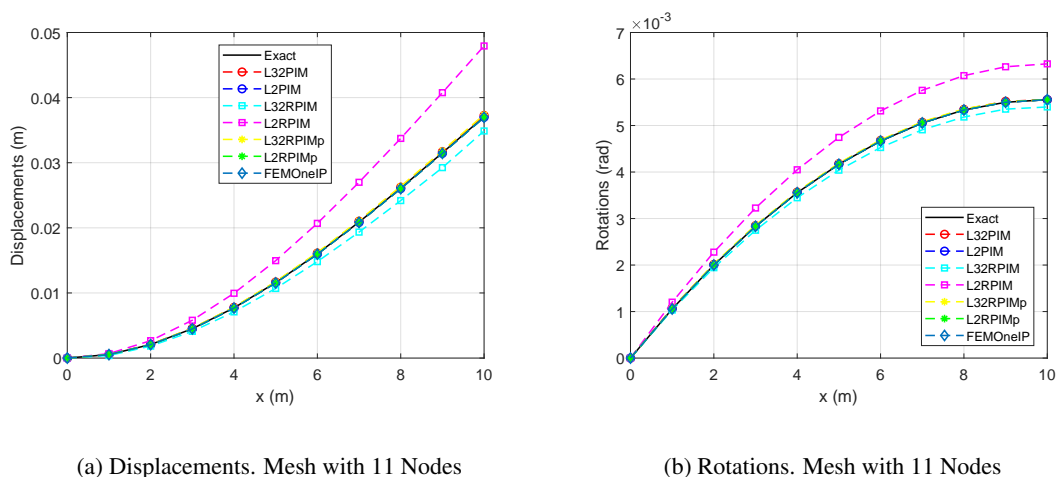
Figure 6

solutions showed a good agreement with the exact solution, except for the case of the L2-RPIM model. The main conclusions that can be drawn here are that: (i) the proposed S-PIM models are locking-free, (ii) the L2-PIM and L2-RPIMp models reproduces the results of the linear FEM, and (iii) the L32-PIM and L32-RPIMp models exhibited an upper bound solution, i.e., they are softer than the exact solution, while the FEM is stiffer.

The error was computed with eq. (17) for eight meshes ranging from 5 to 47 nodes equally spaced by 6. The results are shown in Fig. 7. As already pointed out by the results in terms of displacements and rotations, the L2-PIM and L2-RPIMp models exactly reproduce the results of the linear FEM with one integration point. The RPIM models exhibited the highest levels of error, with varying convergence rates. The L32-PIM and L32-RPIMp models presented a rate of convergence similar to the one of the linear FEM, with an higher error.

4 Conclusions

This paper presented a preliminary investigation on the application of S-PIM meshfree models to the analysis of Timoshenko beams. The results obtained with the numerical simulations pointed out that the proposed approach is locking-free. Depending on the number of support nodes used to build the shape functions, different behaviours can be obtained. Using two nodes (L2-scheme) the same solution of the linear FEM with reduced integration was recovered, while using 3 nodes (L32-scheme) and upper-bound solution was obtained. The latter, however, exhibited higher errors with respect to the linear FEM. The main advantage of the proposed approach with respect to the finite element method is that it does not require a numerical integration along the beam; further studies will be devoted to point out the computational efficiency of the method. Furthermore, the method does not require the evaluation of the jacobian, a feature that should constitute a significant advantage in case of geometrical
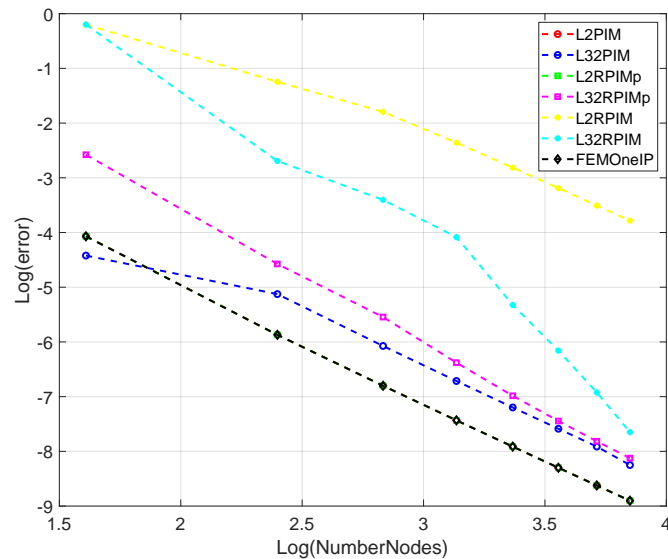
Figure 7. Error norm using displacements and rotations

nonlinearities.

Authorship statement. The authors hereby confirm that they are the sole liable persons responsible for the authorship of this work, and that all material that has been herein included as part of the present paper is either the property (and authorship) of the authors, or has the permission of the owners to be included here.

References

[1] G. Liu, G. Zhang, K. Dai, Y. Wang, Z. Zhong, G. Li, and X. Han. A linearly conforming point interpolation method (lc-pim) for 2d solid mechanics problems. *International Journal of Computational Methods*, vol. 2, n. 04, pp. 645–665, 2005.

[2] G. Zhang and G.-R. Liu. A meshfree cell-based smoothed point interpolation method for solid mechanics problems. In *AIP Conference Proceedings*, volume 1233, pp. 887–892. American Institute of Physics, 2010.

[3] G. Liu and G. Zhang. Edge-based smoothed point interpolation methods. *International Journal of Computational Methods*, vol. 5, n. 04, pp. 621–646, 2008.

[4] G.-R. Liu and G.-y. Zhang. *Smoothed point interpolation methods: G space theory and weakened weak forms*. World Scientific, 2013.

[5] G.-R. Liu. A generalized gradient smoothing technique and the smoothed bilinear form for galerkin formulation of a wide class of computational methods. *International Journal of Computational Methods*, vol. 5, n. 02, pp. 199–236, 2008.

[6] J. Hale. *Meshless methods for shear-deformable beams and plates based on mixed weak forms*. PhD thesis, Imperial College London, 2013.

[7] C. Du, D. Zhang, L. Li, and G. Liu. A node-based smoothed point interpolation method for dynamic analysis of rotating flexible beams. *Acta Mechanica Sinica*, vol. 34, n. 2, pp. 409–420, 2018.

[8] C. He, X. Wu, T. Wang, and H. He. Geometrically nonlinear analysis for elastic beam using point interpolation meshless method. *Shock and Vibration*, vol. 2019, 2019.

[9] G.-R. Liu. *Meshfree Methods: moving beyond the the finite element method*. Taylor & Francis, 2009.

[10] G.-R. Liu. A g space theory and a weakened-weak (w^2) form for a unified formulation of compatible and incompatible methods: Part i theory. *International Journal for Numerical Methods in Engineering*, vol. 81, n. 9, pp. 1093–1126, 2010.